

# Directed Flow of $\Lambda$ -Hyperons in 2 - 6 AGeV Au + Au Collisions

P. Chung<sup>(1)</sup>, N. N. Ajitanand<sup>(1)</sup>, J. M. Alexander<sup>(1)</sup>, M. Anderson<sup>(5)</sup>, D. Best<sup>(3)</sup>, F.P. Brady<sup>(5)</sup>, T. Case<sup>(3)</sup>, W. Caskey<sup>(5)</sup>, D. Cebra<sup>(5)</sup>, J.L. Chance<sup>(5)</sup>, B. Cole<sup>(10)</sup>, K. Crowe<sup>(3)</sup>, A. Das<sup>(2)</sup>, J.E. Draper<sup>(5)</sup>, M.L. Gilkes<sup>(1)</sup>, S. Gushue<sup>(1,8)</sup>, M. Heffner<sup>(5)</sup>, A.S. Hirsch<sup>(6)</sup>, E.L. Hjort<sup>(6)</sup>, L. Huo<sup>(12)</sup>, M. Justice<sup>(4)</sup>, M. Kaplan<sup>(7)</sup>, D. Keane<sup>(4)</sup>, J.C. Kintner<sup>(11)</sup>, J. Klay<sup>(5)</sup>, D. Krofcheck<sup>(9)</sup>, R. A. Lacey<sup>(1)</sup>, J. Lauret<sup>(1)</sup>, M.A. Lisa<sup>(2)</sup>, H. Liu<sup>(4)</sup>, Y.M. Liu<sup>(12)</sup>, R. McGrath<sup>(1)</sup>, Z. Milosevich<sup>(7)</sup>, G. Odyniec<sup>(3)</sup>, D.L. Olson<sup>(3)</sup>, S. Y. Panitkin<sup>(4)</sup>, C. Pinkenburg<sup>(1)</sup>, N.T. Porile<sup>(6)</sup>, G. Rai<sup>(3)</sup>, H.G. Ritter<sup>(3)</sup>, J.L. Romero<sup>(5)</sup>, R. Scharenberg<sup>(6)</sup>, L. Schroeder<sup>(3)</sup>, B. Srivastava<sup>(6)</sup>, N.T.B Stone<sup>(3)</sup>, T.J.M. Symons<sup>(3)</sup>, T. Wienold<sup>(3)</sup>, R. Witt<sup>(4)</sup>, J. Whitfield<sup>(7)</sup>, L. Wood<sup>(5)</sup>, and W.N. Zhang<sup>(12)</sup>  
(E895 Collaboration)

<sup>(1)</sup>*Depts. of Chemistry and Physics, SUNY Stony Brook, New York 11794-3400*

<sup>(2)</sup>*Ohio State University, Columbus, Ohio 43210*

<sup>(3)</sup>*Lawrence Berkeley National Laboratory, Berkeley, California, 94720*

<sup>(4)</sup>*Kent State University, Kent, Ohio 44242*

<sup>(5)</sup>*University of California, Davis, California, 95616*

<sup>(6)</sup>*Purdue University, West Lafayette, Indiana, 47907-1396*

<sup>(7)</sup>*Carnegie Mellon University, Pittsburgh, Pennsylvania 15213*

<sup>(8)</sup>*Brookhaven National Laboratory, Upton, New York 11973*

<sup>(9)</sup>*University of Auckland, Auckland, New Zealand*

<sup>(10)</sup>*Columbia University, New York, New York 10027*

<sup>(11)</sup>*St. Mary's College, Moraga, California 94575*

<sup>(12)</sup>*Harbin Institute of Technology, Harbin, 150001 P. R. China*  
(August 20, 2019)

Directed flow measurements for  $\Lambda$  - hyperons are presented and compared to those for protons produced in the same Au + Au collisions (2, 4, and 6 AGeV;  $b < 5-6$  fm). The measurements indicate that  $\Lambda$  - hyperons flow consistently in the same direction and with smaller magnitudes than those of protons. Such a strong positive flow [for  $\Lambda$ s] has been predicted in calculations which include the influence of the  $\Lambda$ -nucleon potential. The experimental flow ratio  $\Lambda/p$  is in qualitative agreement with expectations ( $\sim 2/3$ ) from the quark counting rule at 2 AGeV but is found to decrease with increasing beam energy.

PACS 25.70.+r, 25.70.Pq

A pervasive theme of current relativistic heavy ion research is the creation and study of nuclear matter at high energy densities [1–4]. Central to these studies are questions related to how hadronic properties may be modified in a hot and dense nuclear medium [5,6]. Modifications to the properties of  $\Lambda$ 's and kaons which influence their production and propagation are of particular current interest [5,7–13]. This is because they have not only been linked to a chirally restored phase of nuclear matter [5], but also to the detailed characteristics of the high density nuclear material existing in neutron stars [14,15].

Recent theoretical studies of the propagation of  $\Lambda$ 's and kaons, in hot and dense nuclear matter, have identified characteristic flow patterns for these particles which could serve as an important probe for their respective in-medium potentials [9,10,12,13]. Subsequently, results from kaon measurements have been attributed to the in-

fluence of the vector component of the in-medium kaon-nucleon potential [16–18]. The propagation of  $\Lambda$ 's [in nuclear matter] is predicted to differ from that of kaons due to these different interactions. For example, at relatively low energies the  $\Lambda$ -nucleon scattering cross section is much larger than the kaon-nucleon cross section. More importantly, the kaon potential is thought to be weakly repulsive while that for  $\Lambda$ -hyperons is believed to be attractive for the conditions expected in 1-10 AGeV heavy ion collisions [12]. One of the possible manifestations of these differences is a predicted pattern for directed flow of  $\Lambda$ 's which is distinguishable from that for kaons and protons [9,12,13]. Theoretical studies of the directed flow of  $\Lambda$ 's show that the  $\Lambda$  flow is relatively insensitive to the magnitude of the  $\Lambda$ -nucleon cross section, but has greater sensitivity to the  $\Lambda$ -nucleon potential [9,12]. Thus, it is important to obtain a set of  $\Lambda$  flow measurements in the 1-10 AGeV beam energy range and to test its utility as an important constraint for the  $\Lambda$ -nucleon potential.

In this letter, we present the first experimental flow excitation function for  $\Lambda$  - hyperons at AGS energies, and compare it to that for protons produced in the same Au + Au collisions. These measurements are important because they provide a unique opportunity for probing the  $\Lambda$ -nucleon potential in collisions which are predicted to produce the highest baryon densities [19]. Such an opportunity is not afforded by hypernuclei studies which allow the investigation of the  $\Lambda$ -nucleon potential at or below normal nuclear matter density. Knowledge of the  $\Lambda$  - nucleon potential at high baryon densities is crucial for accurate predictions of the amount of strangeness-bearing matter in the interior of neutron stars [20]

Measurements have been performed with the E895

detector system at the Alternating Gradient Synchrotron at the Brookhaven National Laboratory. Details on the detector and its setup have been reported earlier [18,22,23]. Suffice it to say, the data presented here benefit from the excellent coverage, continuous 3D-tracking, and particle identification capabilities of the TPC. These features are crucial for the efficient detection and reconstruction of  $\Lambda$ 's and for accurate flow determinations.

The  $\Lambda$ -hyperons have been reconstructed from the daughters of their charged particle decay,  $\Lambda \rightarrow p + \pi^-$  (branching ratio  $\sim 64\%$ ) following the procedure outlined in Refs. [18] and [24]. All TPC tracks in an event were reconstructed followed by the calculation of an overall event vertex. Thereafter, each  $p\pi^-$  pair was considered and its point of closest approach obtained. Pairs whose trajectories intersect (with fairly loose criteria such as decay distance from event vertex  $> 0.5$  cm) at a point other than the main event vertex were assigned as  $\Lambda$  candidates and evaluated to yield an invariant mass and associated momentum. These  $\Lambda$  candidates were then passed to a fully connected feedforward multilayered neural network [26] trained to separate “true”  $\Lambda$ 's from the combinatoric background. The network was trained from a set consisting of “true”  $\Lambda$ 's and a set consisting of a combinatoric background. “True”  $\Lambda$ 's were generated by tagging and embedding simulated  $\Lambda$ 's in raw data events in a detailed GEANT simulation of the TPC. The combinatoric background or “fake”  $\Lambda$ 's were generated via a mixed event procedure in which the daughter particles of the  $\Lambda$  ( $p\pi^-$ ) were chosen from different data events.

The invariant mass distributions for  $\Lambda$ 's obtained from the neural network are shown in Figs. 1a - 1c for 2, 4, and 6 AGeV Au + Au collisions respectively [27]. It is noteworthy that we have verified that the procedure used to train the neural network does not lead to the spurious “creation” of  $\Lambda$ 's (see Ref. [18]). That is, combinatoric background processed through the neural network does not lead to  $\Lambda$  peaks in the invariant-mass distribution as demonstrated for 6 AGeV data in Fig. 1d.

The distributions shown in Fig. 1 have been obtained for central and mid-central events in which one or more  $\Lambda$ 's have been detected. Using the charged particle multiplicity of an event as a measure of its centrality, we estimate that these events are associated with an impact-parameter range  $b \lesssim 5-6$  fm. The distributions shown in Figs. 1a - 1c show relatively narrow invariant mass peaks (Full Width at Half Maximum  $\sim 6$  MeV) at the characteristic value expected for the  $\Lambda$  hyperon ( $\sim 1.116$  GeV). The distributions also show an excellent peak to background ratio which clearly attests to the reliability of the separation from combinatoric background.

Fig. 1e shows a typical decay-length distribution (in the c.m. frame) for  $\Lambda$ 's obtained at 6 AGeV. A deficit below  $ct \sim 20$  cm reflects the difficulty of  $\Lambda$  reconstruction in the region of high track density near to the main event vertex. Deficiencies above 40 cm reflect inefficiencies associated with  $\Lambda$  decays close to the edge of the TPC. An

exponential fit to the distribution over a region for which the detection efficiency is constant ( $\sim 22 - 38$  cm), yields a  $c\tau$  value of  $7.9 \pm 0.1$  cm ( $\chi^2 \sim 0.9$ ). This value is close to the expected value of 7.8 cm.

A better appreciation of the TPC coverage can be obtained from the  $P_t$  vs rapidity plot (cf Fig.2) obtained for 4 AGeV  $\Lambda$ 's. One can identify 2 areas of low acceptance: (1)  $P_T < 100$  MeV, due to the high track density in a cone around the beam, (2) rapidity  $< -0.6$ , due to the finite volume of the TPC. These two types of losses exhibit different trends with beam energy. The first one is least prominent at 2 AGeV and becomes gradually worse at 6 AGeV due to the higher track density. The second one is worst at 2 AGeV but improves gradually with increasing beam energy as a result of the increasing nucleon-nucleon c.m. rapidity with beam energy.

The method for analysis of the sideward flow of protons has been discussed in a prior publication [28]. Here we focus only on the procedure employed for  $\Lambda$ 's. The hatched area centered on the invariant mass peaks shown in Figs. 1a - 1c ( $1.11 \leq m_{inv} \leq 1.122$ ) represents the mass gates used for the flow analysis. These gates ensure a relatively pure sample of  $\Lambda$ 's ( $\sim 90\%$ ) for all beam energies. On the other hand, this sample may include secondary  $\Lambda$ 's which result from the decay of  $\Sigma^0$ 's. These secondary  $\Lambda$ 's are experimentally indistinguishable [via our analysis] from the primary ones but it is believed that they do not constitute the bulk of the detected  $\Lambda$ 's. Results from the Relativistic Quantum Molecular Dynamics model [29] indicate; (a) a maximum ratio  $\Sigma^0/\Lambda$ , of  $\sim 0.3$  for the 2 - 6 AGeV Au + Au collisions relevant to our analysis and (b) a  $\Sigma^0$  flow magnitude which is similar to that for  $\Lambda$ 's.

The reaction plane was determined via the standard transverse momentum analysis method of Danielewicz and Odnyciec [30] as described in detail in Ref. [23]. We note here that the daughter protons of  $\Lambda$  candidates were excluded from the proton sample used for reaction plane determination. Such a procedure eliminates any auto-correlation. Deficiencies in the acceptance of the TPC result in a non-uniform reaction plane distribution for all beam energies. We account for such non-uniformities by applying rapidity and multiplicity dependent corrections [23] which serve to flatten the reaction plane distribution. The dispersion of the reaction plane was estimated for 2,4 and 6 AGeV via the the sub-event method [30]; values of the dispersion correction are 1.08, 1.20 and 1.44 respectively [23].

Figs. 3a - c show representative results for the mean transverse momenta in the reaction plane  $\langle p^x \rangle$ , vs. the normalized c.m. rapidity  $y_0$ , for protons and  $\Lambda$ 's produced in the same events.  $y_0 = y_{Lab}/y_{cm} - 1$ , where  $y_{Lab}$  and  $y_{cm}$  represent the rapidity of the emitted particle in the Lab and the rapidity of the c.m. respectively. The  $\langle p^x \rangle$  values shown in Fig. 3 have been corrected for reaction plane dispersion [31–33] by the above multiplicative correction factors. The values for the  $\Lambda$ 's also take account of a small correction associated with the  $\sim 9\%$  combinatoric background at each beam energy. The lat-

ter correction was made by evaluating the  $\langle p^x \rangle$  for the experimental combinatoric background [for each of several rapidity bins for each beam energy] followed by a weighted subtraction of these values from the  $\langle p^x \rangle$  values obtained for the invariant mass selections indicated in Fig. 1 (The background flow is consistent with expectations for the uncorrelated proton pion pairs).

Figs. 3a - c show trends which clearly indicate that  $\Lambda$ 's and protons flow consistently in the same direction. However, the magnitude of the  $\Lambda$  flow is consistently smaller than that for protons. These results are consistent with prior  $\Lambda$  - flow measurements [16,24] performed for beam energies  $\lesssim 2$  A GeV. However, they are in stark contrast to the anti-flow pattern recently observed for  $K_s^0$  mesons at 6 A GeV [18]. This contrast is suggestive of differences in the kaon-nucleon and  $\Lambda$ -nucleon potentials. Namely, for a similar range of densities and momenta, the predicted kaon-nucleon potential is repulsive while that for the  $\Lambda$ -nucleon is attractive [9,12,13].

In order to quantify the flow magnitude we have evaluated the slope at mid-rapidity for protons  $F_p$  and  $\Lambda$ 's  $F_\Lambda$  ( $F_{p,\Lambda} = \frac{d\langle p^x \rangle}{dy_0}|_{(y_0 \sim 0)}$ ) of the transverse momentum data (cf. Figs. 3) . The results obtained from linear fits to these data are summarized in Figs. 4a and 4b. Experimental and calculated  $\Lambda$  flow excitation functions are shown in Fig. 4a; the data and the results from RQMD ( $v$  2.3) [29] calculations both indicate a continuous decrease in the flow ( $F$ ) with increasing beam energy. However, the results from the calculation systematically underpredict the experimentally observed flow magnitude. Since rescattering effects are included in the RQMD calculations, it is suggested that the difference may be due to the absence of the  $\Lambda$ -nucleon potential in RQMD. It is important to point out here that stronger  $\Lambda$  flow has been found in calculations which include the explicit effect of the  $\Lambda$  nucleon potential [9,12,13].

The observed trend of the  $\Lambda$  flow is very similar to that observed for protons co-produced with  $\Lambda$ 's, as well as for protons in which no explicit condition for  $\Lambda$  detection was imposed [28]. The decrease of  $F$  with increasing beam energy is consistent with the notion that the flow of primordial  $\Lambda$ 's reflects the collective flow of the baryon-baryon and pion-baryon pairs from which they are produced. This trend could also result from a weakening of rescattering effects and/or the attractive  $\Lambda$ -nucleon potential. Such a weakening of the  $\Lambda$ -nucleon potential has been predicted for relatively large baryon densities [12].

The quark counting rule asserts that  $\Lambda$ 's interact with nucleons only through their non-strange quark constituents [25]. Since a  $\Lambda$  particle has only two such quarks, this suggests that the  $\Lambda$  potential is  $\sim 2/3$  of that for nucleons [25]. The experimental flow ratio  $F_\Lambda/F_p$ , is shown as a function of beam energy in Fig. 4b. The data indicate a value of  $\sim 2/3$  at 2 AGeV. This value is similar to that obtained for the Ni + Cu system [24], and is in qualitative agreement with the suggested ratio of the  $\Lambda/p$  potential. On the other hand, there is an unmis-

takeable deviation from the value  $2/3$  (indicated by the dashed line) with increasing beam energy. Such a deviation suggests that a simple scaling by  $2/3$  to obtain the  $\Lambda$ -nucleon potential may be an oversimplification. The deviation could be related to rescattering effects or to the detailed characteristics of the  $\Lambda$ -nucleon potential for the densities produced at 4 and 6 A GeV. More detailed calculations are required to distinguish between these two effects.

We have measured directed flow excitation functions for  $\Lambda$ -hyperons and protons produced in the same mid-central Au+Au collisions. The data show positive flow for  $\Lambda$ 's and protons for all beam energies. This observation is in stark contrast to the prominent anti-flow observed for neutral kaons from the same data set [18]. This contrast is suggestive of the expected differences in the kaon-nucleon and  $\Lambda$ -nucleon interactions for the densities attained in 2 - 6 AGeV Au + Au collisions. A comparison of the  $\Lambda$  flow excitation function to that obtained from RQMD, shows consistently larger experimental values, suggesting an influence of the  $\Lambda$ -nucleon interaction. Both  $\Lambda$  and proton flow show a decrease with increasing beam energy. However, the flow ratio  $F_\Lambda/F_p$ , decreases from  $\sim 2/3$  at 2 AGeV to  $\sim 1/3$  at 6 AGeV. Such a trend is qualitatively inconsistent with the quark counting rule and could be related to the detailed features of the  $\Lambda$ -nucleon potential. More studies of strange particle dynamics can illuminate additional properties of high density matter which is thought to be rich in strangeness.

This work was supported in part by the U.S. Department of Energy under Grant No. DE-FGO2-87ER40331.A008 and other grants acknowledged in Ref. [23]. We acknowledge fruitful discussions with M. Prakash.

- 
- [1] H. Stocker and W. Greiner, Phys. Rep. 137, 277, (1987).
  - [2] *Quark Matter '99*, Nucl. Phys. A661, (1999)
  - [3] W.Reisdorf,H.Ritter,Ann.Rev.Nuc.Par.Sci.47,663 (1997)
  - [4] S. A. Bass et al., J. Phys. G 25:R1 (1999)
  - [5] G. E. Brown et al., Phys. Rev. C43, 1881, (1991).
  - [6] P. Senger and H. Ströbele, nucl-ex/9810007.
  - [7] D. B. Kaplan et al., Phys. Lett. B175, 57 (1986).
  - [8] T. Waas et al., Phys. Lett. B379, 34 (1996).
  - [9] G.Q. Li, C.M. Ko Phys. Rev. C54 1897, (1996).
  - [10] Bratkovskaya et al., Nucl. Phys. A 622, 593, (1997).
  - [11] M. Lutz, Phys. Lett. B 426, 12 (1998).
  - [12] G. Q. Li et al., Nucl. Phys. A636, 487 (1998).
  - [13] Z. S. Wang et al., Nucl.Phys. A645 177, (1999); Erratum-  
ibid. A648 281, (1999).
  - [14] G. Q. Li et al., Nucl. Phys. A625, 372 (1997).
  - [15] V. Thorsson et al., Nucl. Phys. A572, 693 (1994).
  - [16] J. Ritman et al., Z Phys. A352, 355, (1995).
  - [17] Y. Shin et al., Phys. Rev. Lett. 81, 1576 (1998).
  - [18] P. Chung et al., Journal of Phys. G., 25, 255 (1999);

- P. Chung et al., Phys. Rev. Lett 85, 940 (2000).  
 [19] Y. Pang et al., Phys. Rev. Lett. 68, 2743 (1992).  
 [20] M.Prakash, J.Lattimer, Nucl.Phys.A639, 433c (1998).  
 [21] G. Bauer et al., NIM A**386**, 249 (1997).  
 [22] G. Rai et al., IEEE Trans. Nucl. Sci. 37, 56 (1990).  
 [23] C. Pinkenburg et al., Phys.Rev.Lett. 83, 1295 (1999).  
 [24] M. Justice, et al., Phys. Lett. B**440**, 12, (1998).  
 [25] Steven A. Moszkowski, Phys. Rev. D, 1613 (1973)  
 [26] M. Justice, NIM Phys. Res. A 400, 463 (1997).  
 [27] Actual beam energies were 1.85, 3.9 and 5.9 AGeV. Measurements were also made at 7.9 AGeV but these results suffer from rather poor statistics.  
 [28] H. Liu et al., Phys.Rev.Lett. 84, 5488 (2000).  
 [29] H. Sorge, Phys. Rev. C**52**, 3291, (1995).  
 [30] P.Danielewicz, G.Odyniec, Phys.Lett.B157,146 (1985).  
 [31] P. Danielewicz et al., Phys. Rev. C **38**, 120,(1988).  
 [32] J.-Y. Ollitrault, nucl-ex/9711003 v2.  
 [33] A.Poskanzer, S.Voloshin, Phys. Rev C**58**, 1671, (1998).

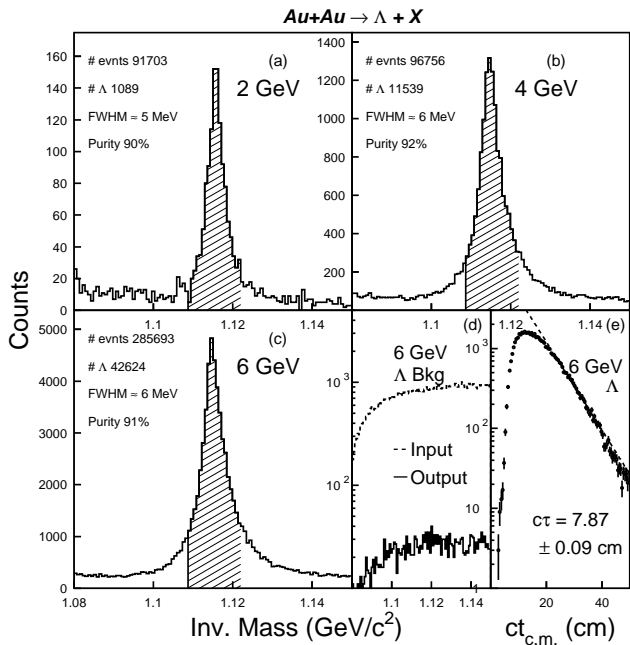


FIG. 1. Invariant mass distribution for  $\Lambda$  hyperons measured at 2, 4, 6 AGeV as indicated ( $b < 6\text{fm}$ ). Panel (d) shows input (dashed curve) and output (solid curve) invariant mass distributions for combinatoric events. Panel (e) shows the decay length distribution.

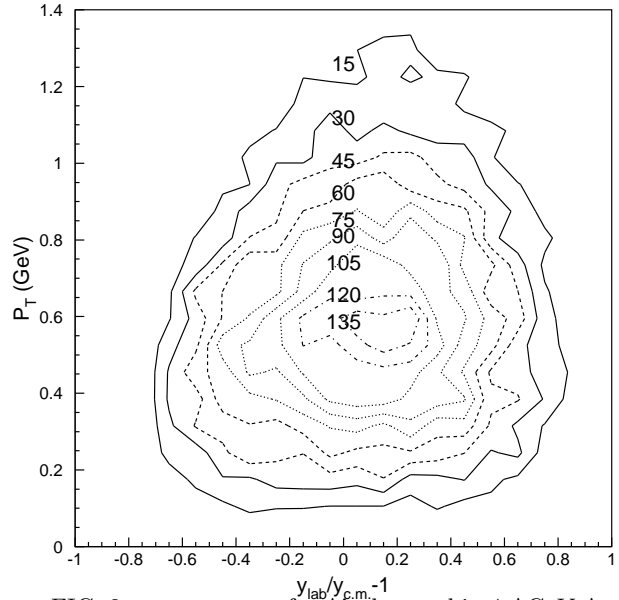


FIG. 2.  $\langle p_T \rangle$  vs  $y_0$  for  $\Lambda$ 's detected in 4 AGeV Au + Au collisions. Contour levels are indicated.

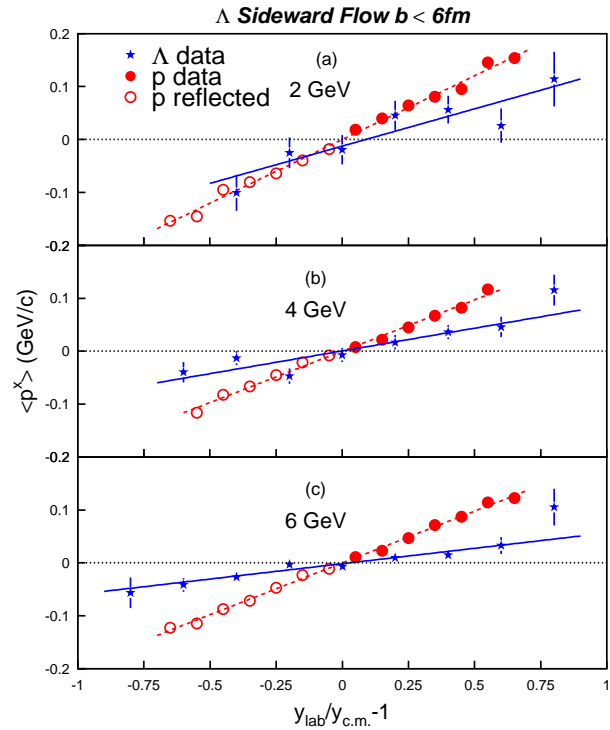


FIG. 3.  $\langle p^x \rangle$  vs  $y_0$  for  $\Lambda$ 's and protons ( $b < 6\text{fm}$ ). The open circles indicate the reflected values for protons, and the solid and dashed-curves represent fits to the data. The  $\langle p^x \rangle$  values are corrected for reaction plane dispersion.

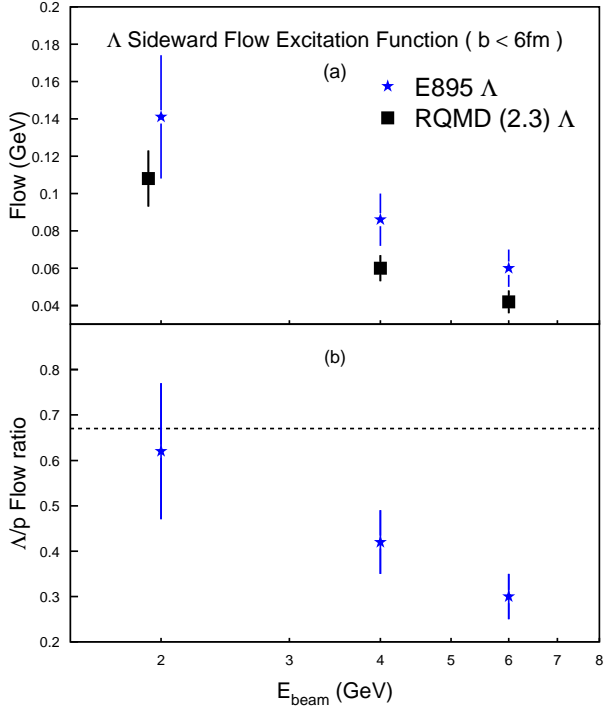


FIG. 4. (a)  $\Lambda$  hyperon flow vs beam energy. Filled stars and squares represent data and RQMD results respectively. (b)  $\Lambda/p$  flow ratio vs beam energy for the same impact-parameter range. The dashed line indicates a value of  $2/3$ .